Thermal Ignition

Introduction

One of the leading hypotheses put forward by the LENR community for potential AHE observations is that the process is driven by a *phonon-mediated* mechanism; in other words, vibrations of atoms within a material could drive deuterons to close enough proximity to undergo fusion. The main experimental "knob" for tuning these atomic vibrations is simply temperature: The amplitude and frequency of these vibrations and motion of the atomic lattice is known to scale exponentially with increasing temperatures[23]. While, in theory, this is a straight-forward process (there are many ways to heat a material to extreme temperatures), doing so in a controlled manner that allows for studying and looking for potential AHE events is significantly more difficult.

Our Thermal Ignition campaign focuses on the development of systems that can deliver *rapid and intense* temperature rises to a loaded Pd sample while maintaining the ability to have extreme sensitivity to potential AHE events. In the following text, we will discuss the evolution of this experimental effort as well as a detailed perspective of the final effort, TI-12, that provides unambiguous data supporting that **AHE is not occurring via a thermal stimulation process.** This is shown at temperatures up to and in excess of melting for $PdD_{1.0}$ and $PdH_{1.0}$ (unity loading).

Synopsis of earlier TI campaigns

Our prior experimental campaigns, TI1 – TI11, were focused on the development of an accurate temperature reading under ultra-pressure conditions. In the earliest renditions of TI, we monitored the sample temperature optically by way of pyrometry; this method uses the light emitted from the heated PdD_x sample as a metric of temperature (i.e., consider a "red hot" metal; the amount of light emitted and its color are directly related to the temperature of the metal). Shortly after the start of this campaign, we observed a form of isotopic contrast: Optical pyrometry suggested that the temperature of PdD_x was greatly exceeding the temperature of PdH_x under identical stimulation conditions. Ultimately, we determined that this difference in measured temperature is an artifact unique to ultrapressure environments. Generally, symmetric molecules such as H_2 and D_2 do not absorb light due to a lack of dipole moment. However, at sufficiently high densities/pressures, these molecules collide frequently enough to *temporarily* gain a dipole moment; this process, called collision-induced absorption, is highly sensitive to the mass of the atoms composing the molecule. In other words, the 2x difference in mass between H_2 and D_2 led to different amounts of

[23] The distribution of these atomic vibrations follows Bose-Einstein statistics, where the number of atoms at an energy level, E, scales as $\propto \exp(-E/kT)$.

light absorption at the wavelengths that are used for optical pyrometry, thus causing the observed isotopic contrast and obfuscating our ability to resolve potential AHE events.

To bypass this limitation, we developed ultrapressure electrical feedthroughs to allow for in-situ thermometers. This allowed us to accurately quantify the sample temperature by way of a thermocouple which is known to be insensitive to gaseous environments and negligibly change readout due to pressure. This major hardware upgrade for TI ultimately led to several other campaigns that became greatly improved with the option of electrical feedthroughs for our ultrapressure vessels.

With thermocouples for temperature readouts, we again observed isotopic contrast between measurements under 150 ksi D_2 and H_2. Specifically, we found that PdD_x was heated to a significantly higher temperature than PdH_x under identical stimulation conditions. To confirm whether this effect was due to AHE events or chemical in origin, we performed identical experiments using a material that does not load – Platinum – and is therefore not AHE active. With an identical sample geometry, we confirmed that the peak temperature difference that we initially observed with loaded Pd was repeatable in our Pt control. This observed isotopic contrast was attributable to the difference in cooling power between the two gases; under identical pressures, H_2 cools more effectively than D_2, thus explaining the reduced temperature in PdH_x relative to PdD_x.

In our TI 11 campaign we established the reliability of our *in situ* ultrapressure temperature measurements. This campaign notably deviated from the transient heating protocol we established in all other TI campaigns, instead we investigated high temperature equilibrium loading conditions in PdD and PdH at high pressures. So rather than exploiting a transient state where we are heating faster than we can deload, like in our prior campaigns (and TI12), in TI 11 we sustained an equilibrium state up to the melting point of the material. We were interested at looking at this uncharted territory of keeping a sample at higher temperatures with the resulting lower loadings and exploring the result of that tradeoff to see if we observe anything anomalous and interesting. Figure 1 is a schematic of the experimental setup.

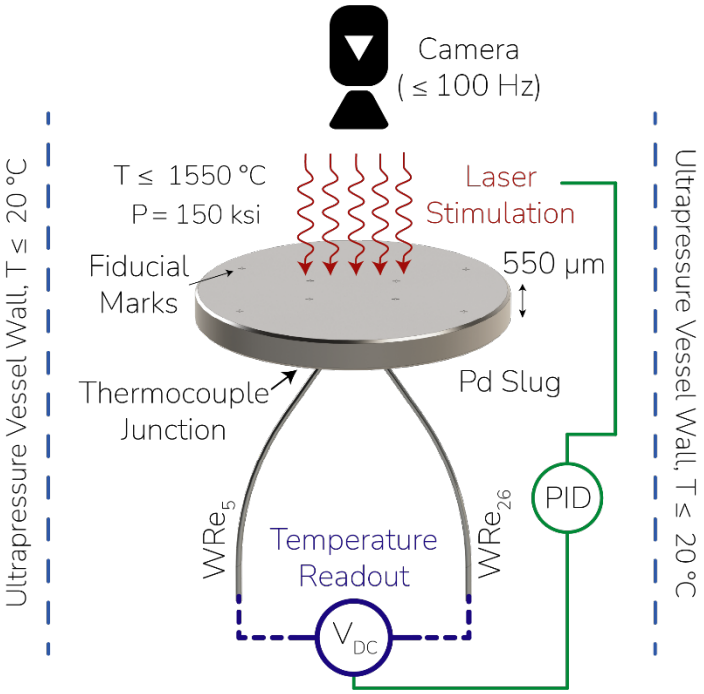

Figure 1: TI-11 Experimental schematic, showing that we are heating by way of a high power laser, in a feedback loop with our thermocouple temperature measurement.

Our TI 11 campaign was the first to melt PdD and PdH under equilibrium conditions, and maintain a melted pool of the PdD/PdH atop the material slug. Initially in our TI 11 campaign we measured a notable difference in the melting point between PdH and PdD. This was later corrected by re-engineering the electrical feedthroughs to remove the inaccurate cold junction compensation offset. Figure 2 below shows the summary of these results, across 13 experiments, showing no significant spread in the measured melting point of PdD and PdH.

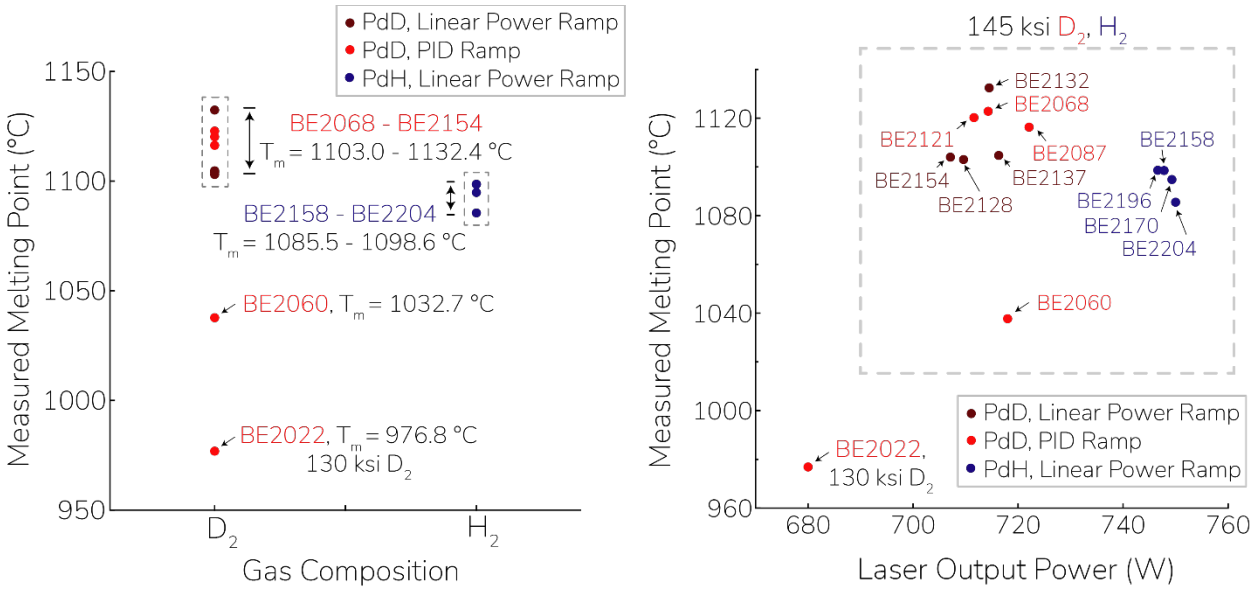

Figure 2: TI-11 campaign summary, showing that we largely eliminated the difference in measured melting point between PdD and PdH.

Unfortunately, no anomalous results were observed in our TI 11 campaign despite holding just below or above the melting temperature for several minutes to hours under ultra pressure conditions. Our last campaign, TI 12, focused on maximizing our resolution, eliminating the need to overcome the rapid cooling of the ultra-pressure deuterium gas to observe an anomalous result.

Thermal Ignition 12 (TI12)

TI12: Advantages and Overview

With experimental data verifying the need for controlled atmospheres (i.e. between the two isotopes), we started our TI12 campaign. This campaign is defined by 3 major aspects relative to prior iterations.

First, TI12 continued to use thermocouples rather than optical measurements to accurately monitor sample temperature. However, in TI11, we observed a significant need for proper cold-junction compensation; in other words, we modified our thermocouples to provide highly accurate temperature measurements, displaying only a few degrees error in the absolute temperature based on known material melting points.

The second major change in TI12 was the introduction of cryogenically cooled samples. This cryogenic cooling allows us to load PdD_x to 100%, stoichiometric conditions even at pressures of only 150 ksi; this was confirmed through multiple mass measurements. Additionally, by cryogenically cooling, we can "lock-in" our loading conditions – to allow for stimulation in

identical environments, TI12 relies on loading the sample under high pressure gas, cooling to <-80 C, and then evacuating the vessel and subjecting the sample to vacuum. Due to the ultra-slow kinetics at these low temperatures, the sample is found to *not* deload from stoichiometry even under these vacuum conditions.

TI12's third, and likely most important, modification was the design and implementation of hermetically sealed microcapsules. Although the environment is void of gas/cooling power differences between isotopes, once the sample is rapidly heated with a laser, it will undergo rapid deloading of the stored gas. This gas expulsion is akin to evaporative cooling: the sample temperature immediately drops. More importantly, this temperature drop occurs at different rates for the two isotopes, causing differences in thermal profiles and peak temperatures. By sealing the 100% loaded PdD_x/PdH_x in a hermetic capsule, we can deliver rapid thermal stimulation and contain the deloaded gas within the capsule. The PdD_x/PdH_x samples will thus cool differently, but the capsule as a whole will not. By monitoring the capsule temperature, there is no net energy loss; we have effectively created an adiabatic (no heat exchange / no mass loss to the environment) system. In addition to minimizing heat loss, these microcapsules are also ideal for measurements of isotopic contrast between H_2 and D_2 gases; we have observed PdH_x and PdD_x to have different optical properties, and the use of a microcapsule allows *equal* absorption of laser power between the two, eliminating this anomalous isotopic contrast. This combination allows for unprecedented resolution of potential AHE events.

Due to the critical importance of each, we discuss the experimental validation of these aspects in more detail below. This is followed by our primary experimental results regarding potential AHE events in this experimental campaign.

TI12: Experiments at cryogenic vacuum conditions

One of the major issues with prior TI campaigns was the gaseous environment. Particularly at ultra-pressure (150 ksi) conditions, H_2 and D_2 have different cooling powers, producing a non-AHE-related isotopic difference between the two. To bypass this, *removing* the environment by surrounding the sample with vacuum is simply the most ideal scenario: The sample is now thermally isolated. To highlight the importance and need for vacuum conditions, consider Fig. 3 below. As shown, not only does high pressure gas cool samples at extremely fast rates (and differing rates for different gases!), but the gas leads to a reduction in peak temperatures at early times. This reduced temperature is indicative of "lost" heat at these timescales. One can easily envision that, should an AHE event occur here, that the AHE-related heat could be lost from this convective cooling.

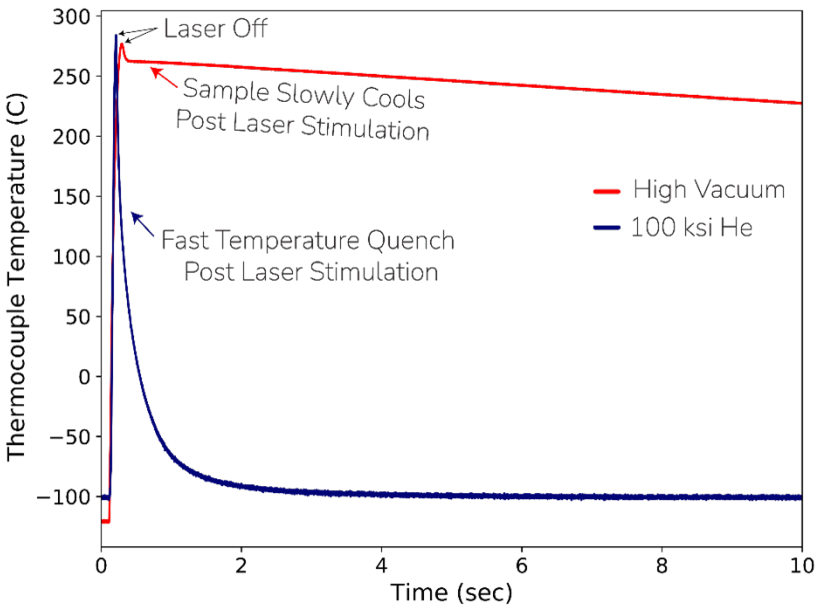

Figure 3: Comparison of temperature profiles following TI laser stimulation of a sample in vacuum (red line) and 100 ksi of He gas (blue line).

While vacuum conditions are thus ideal from an AHE-detection perspective, they are non-trivial to obtain for our samples. Palladium loads (or deloads) hydrogen atoms based on the external pressure: Higher pressures lead to higher loadings. Thus, when *loaded* palladium is exposed to vacuum, the sample will *immediately* begin to deload. As one of the major hypotheses regarding AHE is a need for high loadings, this limitation bottlenecks the scope of our experimental campaign.

To address this, we introduced cryogenic cooling to our sample. By loading the sample at 150 ksi and then cooling to temperatures lower than -80 C, we gain two major benefits in these TI12 experiments. First, at these temperatures, the loaded hydrogen atoms become "locked in" to the Pd lattice; in other words, deloading does not occur at – 80 C. Quantitatively, the loading/deloading kinetics of PdD_x/PdH_x follow the Arrhenius equation, where the rate of deloading, is given by $Rate = A \exp\left(-\frac{E}{RT}\right)$, where A is a constant, E is the activation energy for loading, R is the universal gas constant, and T is the sample temperature. Using the activation energy for Pd-H from literature, Fig. 4 shows the rate of deloading as a function of temperature; one can see that at our cryogenic conditions of approximately 200 K, the kinetics for this deloading go to zero, whereas after stimulation (>1000 K) the rate increases by orders of magnitude.

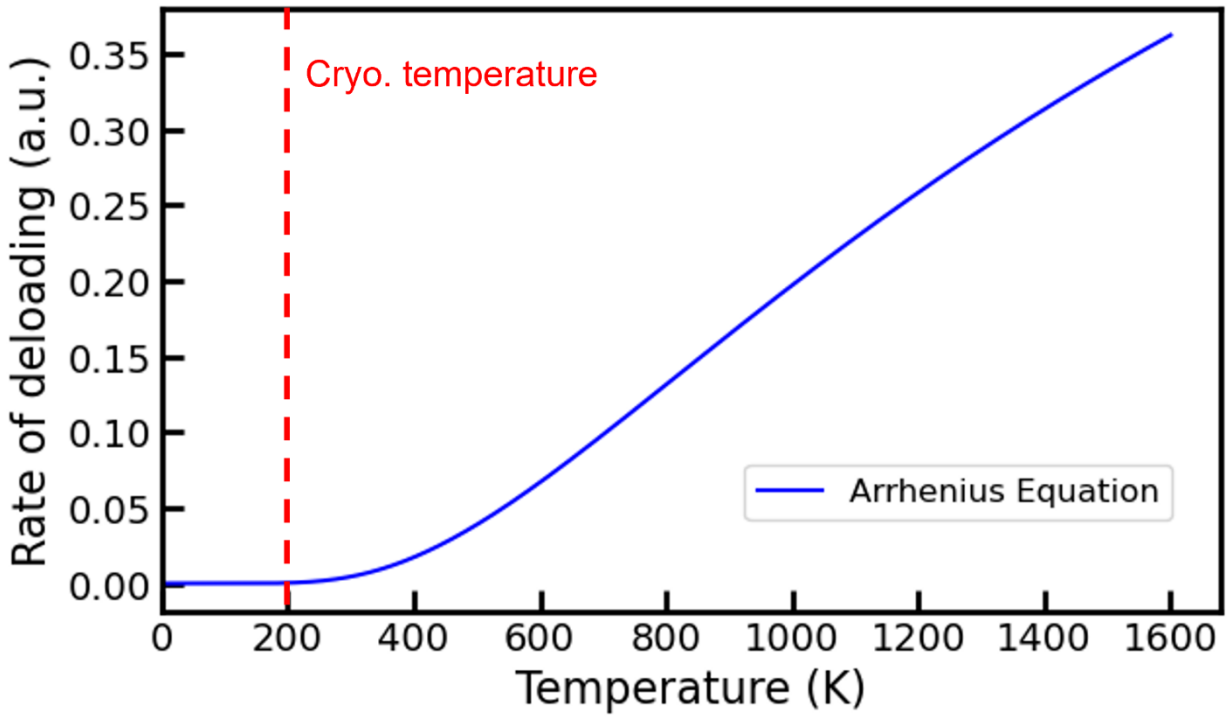

Figure 4: Arrhenius equation for Pd-H highlights the need for cryogenic temperatures to "lock in" loading by reducing the rate of deloading to near-zero at ~200 K.

To further support this, we experimentally verified this critical aspect of our experiment by performing time-resolved loading measurements. As discussed in other sections, the strain, or expansion of the lattice, is directly related to the amount of hydrogen stored within Pd. Thus, we performed experiments in which we monitored the strain during ultrapressure loading, followed by cryogenic cooling and exposure to vacuum. These results are highlighted in Fig. 5 and Fig. 6.

As shown in Fig. 5, we perform a control of these strain measurements by exposing the Pd sample to hydrogen at 150ksi and -100 C for over 24 hours: This provides a direct measure of the error associated with a sample in equilibrium conditions. One can see in the early times of these data that the strain increases upon pressurization and remains constant during this exposure period. Then, after multiple hours and the sample maintained at -100 C, we remove gas from the system and expose the sample to vacuum. As can be seen, for nearly 17 hours, the strain remains unchanged in these cryogenic vacuum conditions. Then, upon heating, deloading occurs and the strain begins to drop.

Figure 6 provides a direct comparison of these temperature-dependent deloading kinetics by comparing the time-resolved strain measurements at -100 C vs. 50 C. At 50 C we observe a gradual reduction in strain while the -100 C sample remains constant. These kinetic rates are in reasonable agreement with the expected Arrhenius-like deloading rates calculated in Fig. 4. Further, we provide a comparison to a Pt control under identical pressure/temperature conditions to highlight

the degree of strain induced by the conditions in the absence of loading; this effect is observed to be negligible relative to the loading-dependent strain in Pd.

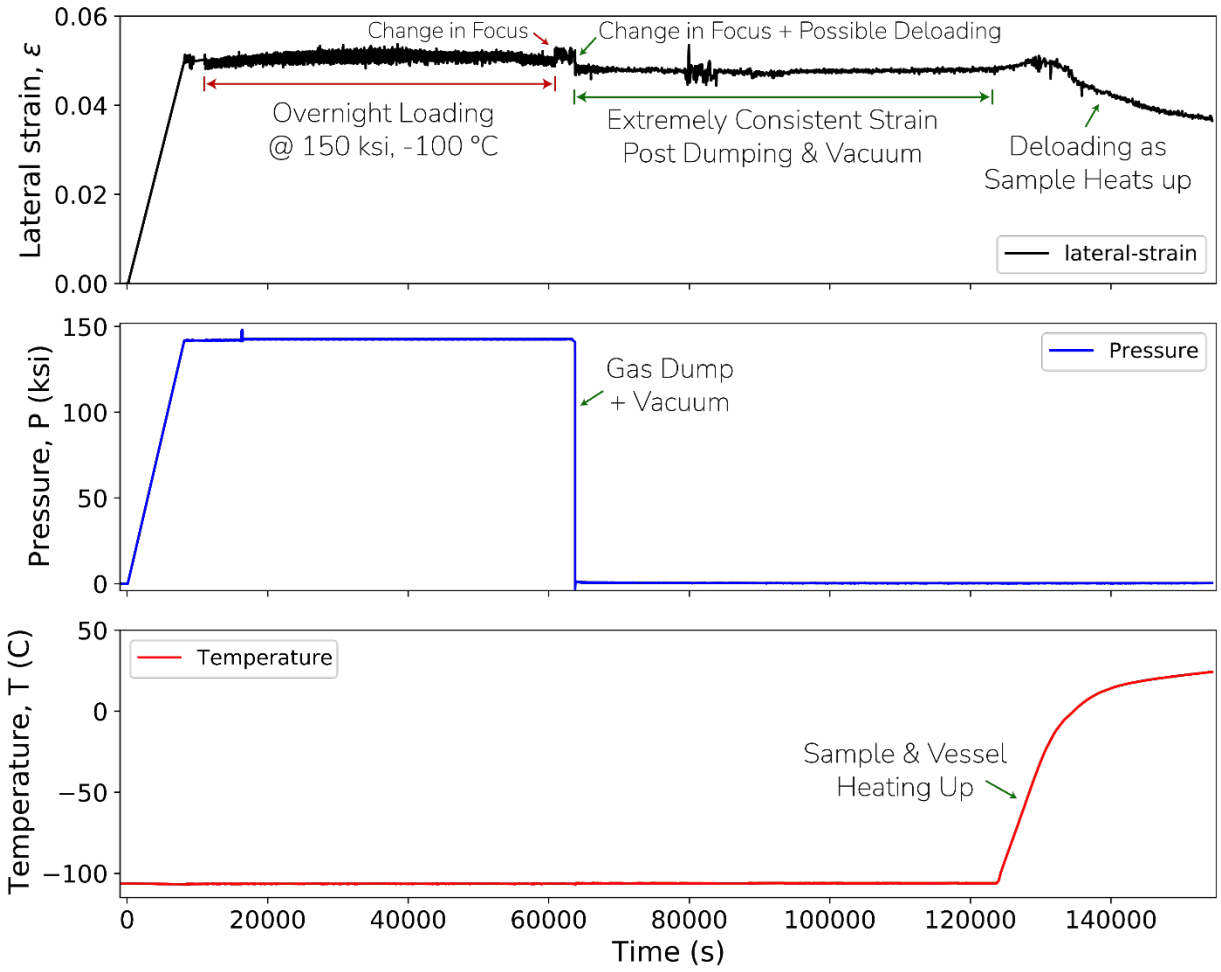

Figure 5: (Top) In-situ strain measurements under varying conditions of gas exposure and temperature. (Middle) Pressure during these strain measurements (Bottom) Temperature during these strain measurements.

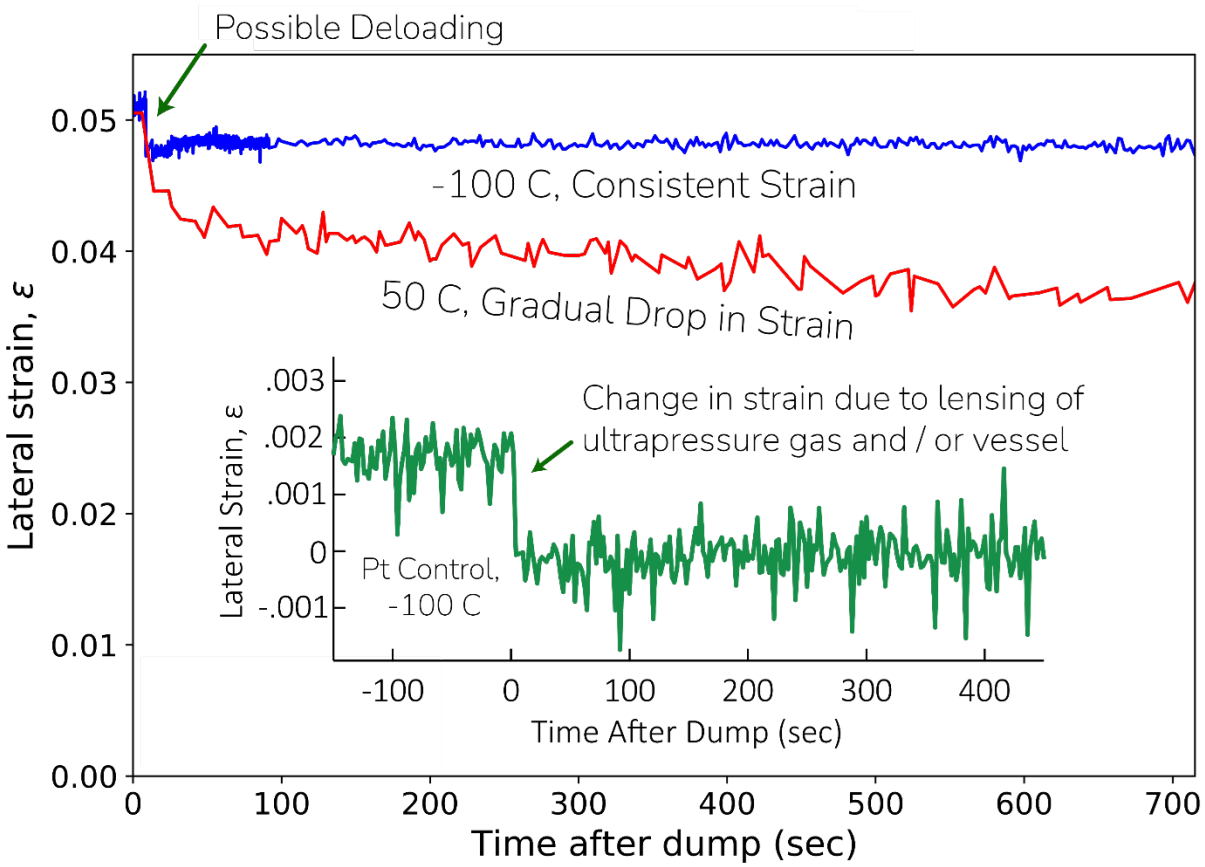

Figure 6: Sample strains for Pd-H exposed to 150ksi hydrogen at -100 C (blue line) and 50 C (red line). A Pt control (green) under identical conditions is shown to highlight the degree of strain induced by pressure alone in the absence of loading.

TI12: Adiabatic microcapsules and thermal isolation

The second major revision introduced for TI12 was the use of microcapsules within our ultra-pressure vessel. These hermetically sealed capsules prevent gas from leaving the system under study and provide adiabatic conditions (no heat loss/mass loss). In doing so, "evaporative" cooling is eliminated from our analysis and thus eliminates anomalous isotopic differences associated with such cooling.

The necessity for *true* hermetic sealing of these capsules, which is an extremely non-trivial task to achieve, can be observed in Fig. 7 below. As shown in Fig. 7, in earlier experiments, we attempted to solve this cooling issue by "capping" the sample in thin, hydrogen-impermeable membranes, namely silicon nitride films. While this approach *significantly* reduced the amount of gas that escapes from the PdDx upon thermal stimulation, we continued to observe a large degree of excessive cooling due to the small amounts of gas molecules escaping. In other words, we experimentally determined that *any* gas escaping from the measurement volume leads to errors in

temperature measurements. Thus, hermetic sealing, or sealing in which no gas escapes, is a *requirement* to test AHE to the highest resolution feasible.

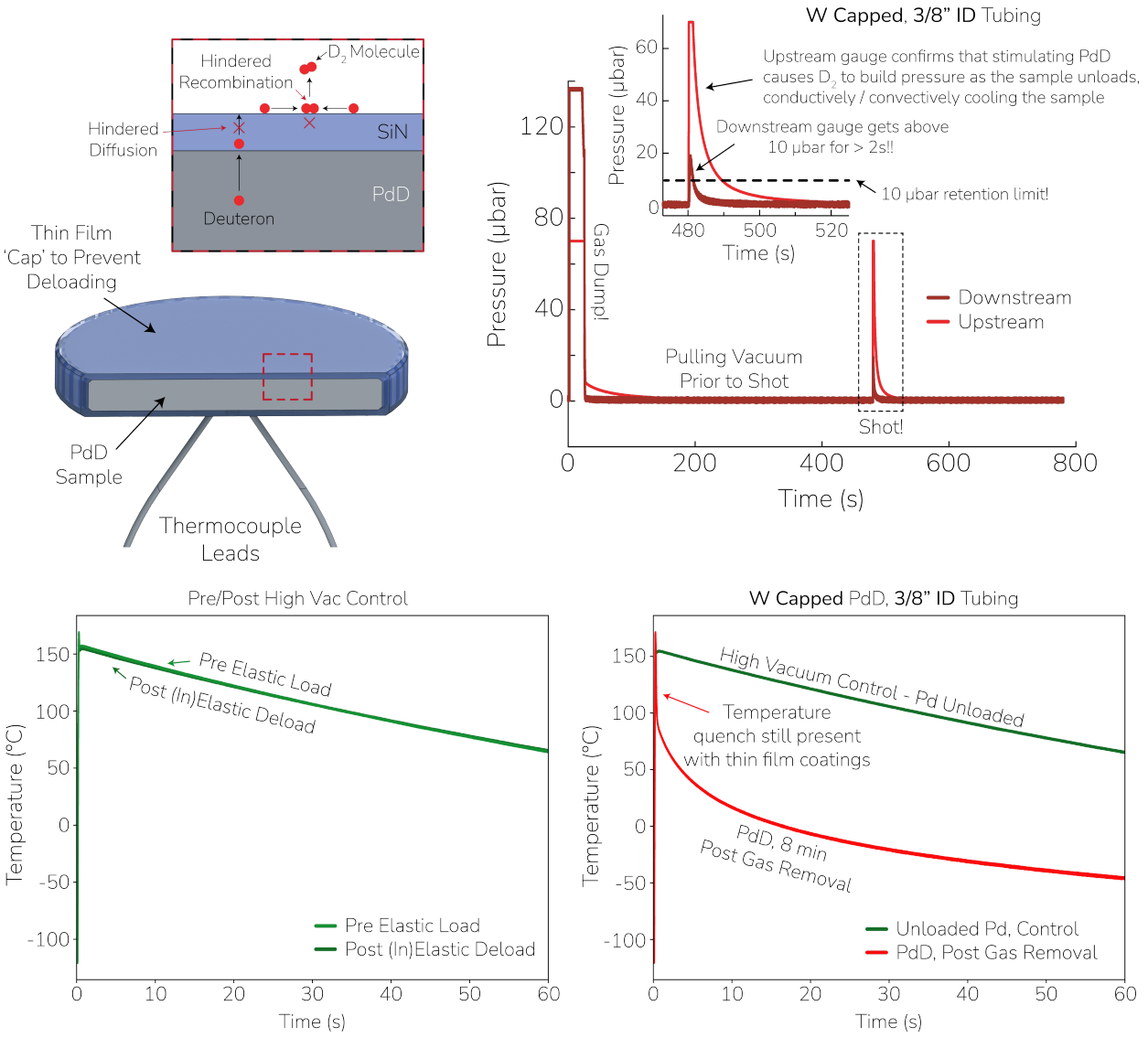

Figure 7: (Top left) Schematic of our SiN-capped Pd samples to attempt to avoid gas deloading. (Top right) Measurements of the gas pressure with the SiN cap relative to the amount of gas lost upon pulling vacuum. (Bottom left) Vacuum controls of unloaded Pd. (Bottom right) Comparison of these vacuum controls to an identically stimulated PdD_x slug. As shown, the SiN cap reduces *quenching, but does not solve the problem.*

The iterations of these microcapsules are shown below in Fig. 8. After multiple experimental cycles, our final design, Gen. 5, provides multiple modifications from earlier iterations that are worth highlighting. First, the capsule is designed in such a way to *maximize* heat transfer between the capsule and the loaded Pd; in TI12, we stimulate the top surface of these capsules and rely on the heat transfer to the underlying Pd to reach the temperatures of interest. By using capsules made

of a MoRe alloy ($MoRe_{0.47}$ wt%), this heat transfer is greatly improved by the high thermal conductivity of MoRe. Notably, MoRe also has a melting temperature of nearly 2500 C, allowing us to stimulate to temperatures in excess of Pd's melting point; MoRe also does not undergo hydrogen loading, thus preventing convective cooling due to its subsequent deloading upon heating. Second, we added and continued improving on various thread designs as a "first-defense" for mechanical stability once the internal pressure spikes following thermal stimulation. This is then supported and made hermetic through an in-house method of laser welding the two components after threading; we found that significant care must be taken in this laser welding process due to the formation of microscale voids that can occur and ultimately lead to premature failure. Notably, when *any* voids were observed following welding, the capsules leaked upon thermal stimulation, despite passing helium leak checks prior to stimulation; in other words, these voids "rupture" due to the excessive heat load supplied by our laser.

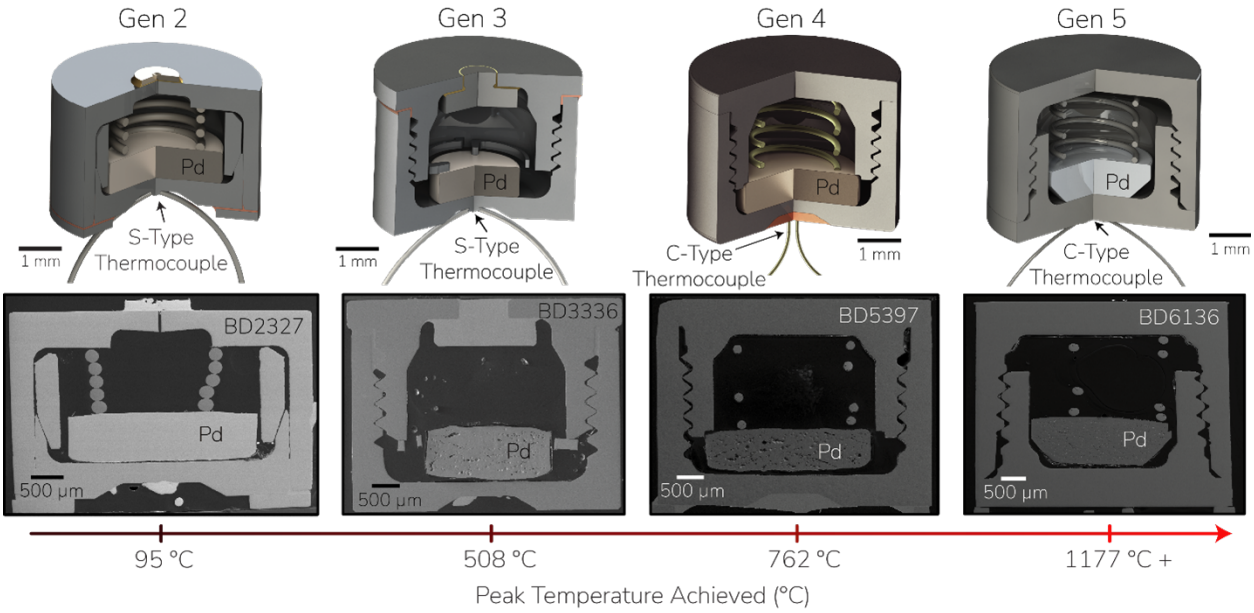

Figure 8: Experimental iterations and improvements on our microcapsules over multiple generations.

In addition to the microcapsule design itself, significant effort was made to ensure true thermal isolation between this capsule and the surrounding pressure vessel. As there is no way to levitate a capsule within a vacuum environment, a mechanical retention is required. This retention must be designed to minimize heat flow between the microcapsule and the pressure vessel itself. To understand the importance of this retention, consider Fig. 9, which shows the iterations of various retention designs and their effect on the temperature distribution. As shown, our final Archimedean spiral provides near the same isolation as expected by true, "perfect" thermal isolation, with only a few percent loss of heat (rather than orders of magnitudes with the prior design!).

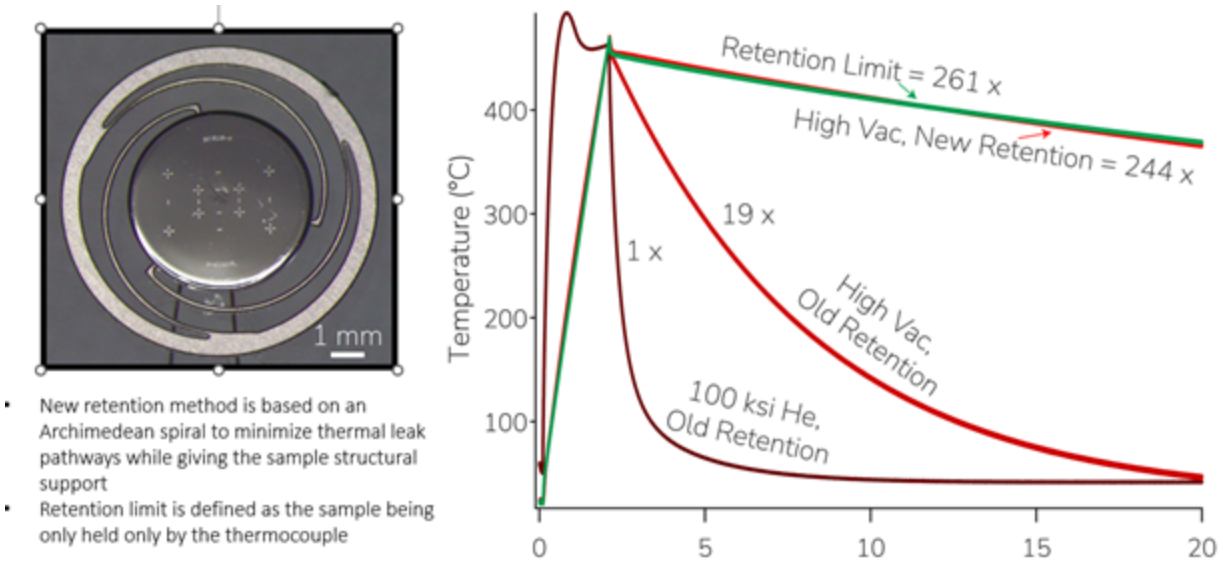

Figure 9: (Left) Final microcapsule retention design for TI12 experiments. (Right) Comparisons of temperature profiles with varying retention designs and "perfect" isolation for comparison. This Archimedean spiral design is within a few percent of the achievable limit, in comparison to our prior retentions that were "leaking" orders of magnitude more heat.

TI12: Experimental protocol and results

With these designs in mind, consider now our experimental protocol: Palladium is placed within a microcapsule and the entire microcapsule assembly is contained within a 150ksi pressure vessel via the Archimedean spiral retention. At this stage, the capsule is entirely sealed (determined by He leak testing) except for a small, 100 μm diameter hole on the front surface; this hole allows gas to enter the capsule for loading.

Prior to loading the Pd, we subject the sample to vacuum, reaching approximately 10^{-7} Torr. With an unloaded Pd sample, we stimulate the sample with a given laser profile (this is varied through our experiments, but generally is a 10 ms pulse that reaches temperatures in excess of Pd melting) and measure the resultant temperature profile. This temperature profile acts as our control. This control is performed for *all* D_2 and H_2 experiments; small changes in microcapsule or Pd mass can lead to large changes in the observed temperature. Thus, our unloaded sample acts as the ideal comparison.

With the experimental control now obtained for a given sample, we load the Pd sample by exposing it for long durations (~hours) to 150ksi D_2/H_2 to ensure homogeneous loading throughout the bulk of the material. Once the Pd is homogeneously loaded, we *slowly* cool the vessel from 25 C to -100 C; by moderating the rate of which we cool the sample, there is sufficient time for *increased* loading to occur at these cryogenic temperatures. These cooling rates are confirmed to be valid for achieving stoichiometric, 100% loading by performing mass measurements of the microcapsule

before and after cooling. This is done by mimicking our TI12 protocol except for stimulation: The capsule is simply removed, and its mass compared to that without loading.

With the vessel now at -100 C, deloading of the sample is inhibited, allowing us to introduce vacuum to the vessel. This first step removes the 150ksi gas and replaces the environment with ~200 psi of D_2. In this relatively low-pressure environment, we perform *in situ* laser welding of the 100- µm hole to finalize the hermetic sealing of the capsule. The slight pressurization, rather than true vacuum, eliminates debris formation from evaporation of the melt pool during this weld step; we observed that true vacuum leads to our laser window becoming obscured and causing anomalous changes in temperature profiles due to reduced light reaching the microcapsule.

With the capsule now sealed, we remove the external 200 psi of D_2/H_2 and again pull true vacuum on the system, reaching identical vacuum to our original control stimulation conditions. At this point, the Pd is 100% loaded with a hydrogen isotope and under identical environmental conditions to our pre-experiment control. Then, we apply same the laser stimulation as our control and compare the two temperature profiles.

A schematic of our final microcapsule design along with representative data of this experimental procedure is shown in Fig. 10 below. In this case, the two stimulation shots are observed to be within 50 C of each other; this small reduction for PdD is also observed for PdH and is attributed to the change in heat capacity due to the increased mass (loaded hydrogen) within the microcapsule volume relative to the control shot. One major takeaway from these data is that the control and loaded PdD cool at *identical* rates, a key benefit of the hermetically-sealed microcapsules that we have designed.

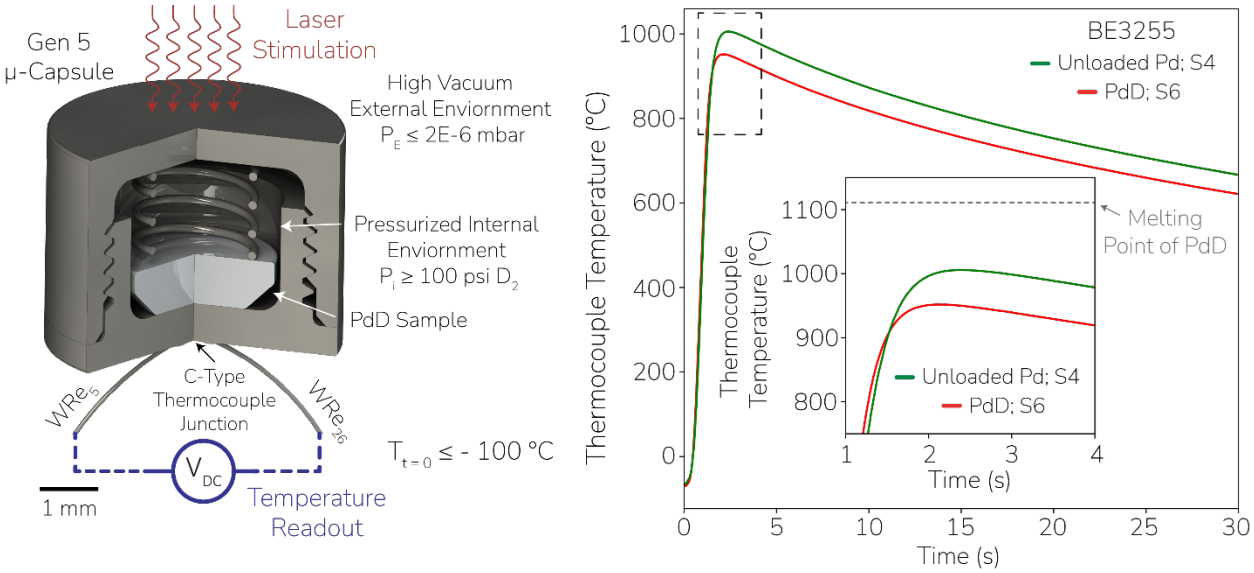

Figure 10: (Left) Schematic of our TI12 microcapsule with laser stimulation and thermocouple readouts. (Right) Representative temperature profiles following stimulation for (green) unloaded Pd, which acts as our control, and (red) stoichiometric PdD after our loading and capsule sealing protocol.

To further extend the stimulation conditions to the "maximum limit," we continued to increase our stimulation conditions until we exceeded the melting temperature of PdD. In Fig. 11 below, we show both the pressure profiles, representative of the degree of evaporative cooling that is experienced by the microcapsule, along with the temperature profiles following stimulation. As observed with lower stimulation conditions, loaded PdD continues to show *lower* temperature excursions than our unloaded Pd control, suggesting an absence of AHE heat input.

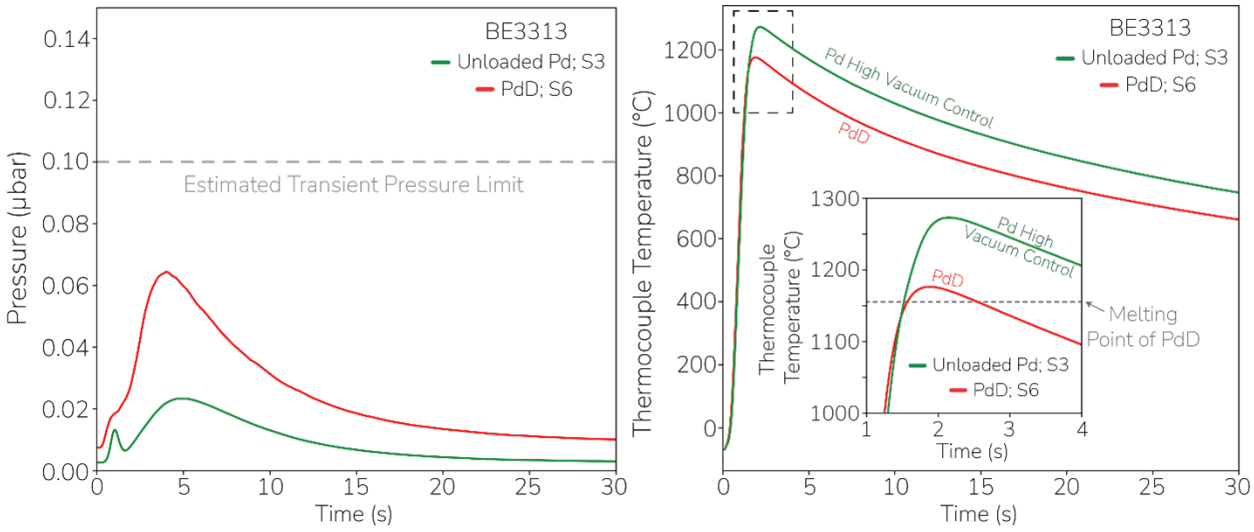

Figure 11: (Left) Transient pressure data following stimulation for (red) PdD and (green) our control. The slight increase in PdD is due to adsorbed gas species as the sample is held at cryogenic conditions. (Right) Temperature profiles following stimulation; both profiles are observed to be in excess of the melting point of PdD. Again, we observe PdD having a lower *temperature rise than the control shot, suggesting a lack of excess heat production.*

To verify melting was achieved, we cross-section the microcapsule after the experiment, allowing us to observe the Pd structure after stimulation was performed. An example of this SEM data is shown below in Fig. 12. The signature of melting here is the large deformation of the Pd itself: The palladium is found to have melted and conformed to the surrounding microcapsule, rather than retaining its original shape. In addition to this clear observation that melting occurred, we note the internal microstructure of the Pd contains large (~25 μm) voids due to the rapid deloading of hydrogen gas during stimulation. These features are consistent in both PdH and PdD experiments.

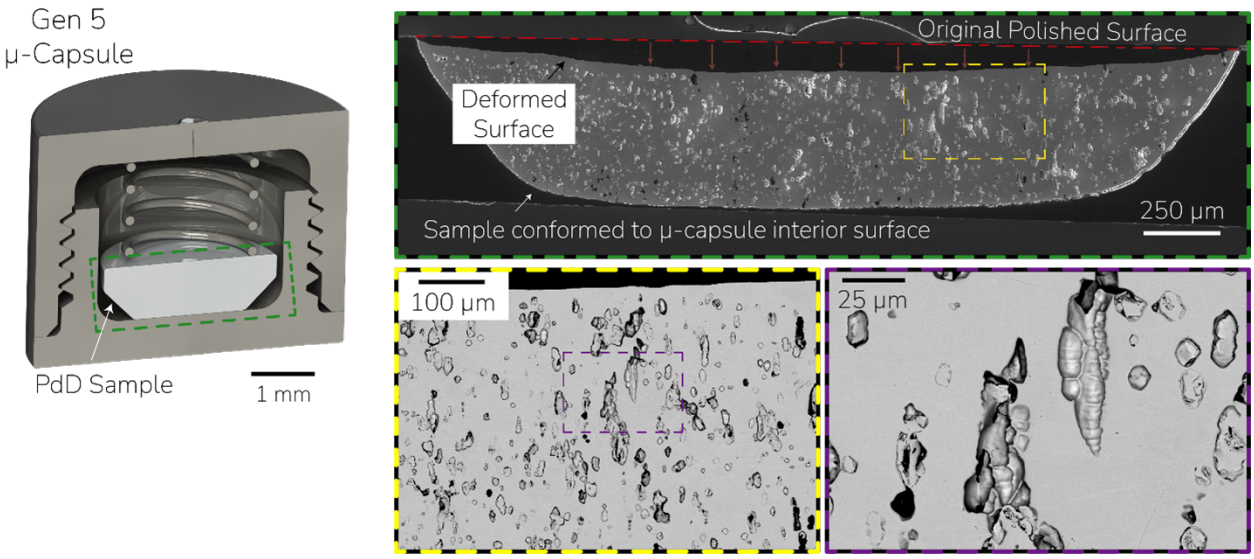

Figure 12: (Left) Microcapsule with the green dashed line representing the cross-sectioned area. (Right, top) SEM micrograph of this dashed region. The Pd is observed to have conformed to the surrounding capsule and collapsed inwards, highlighting that melting occurred during laser stimulation. (Right, bottom) Micrographs of the voids that are formed due to the rapid release of hydrogen gas. These microstructural features are observed for both PdD and PdH.

TI12: Overview and conclusions

Experiment ID (BE####)	**Material (at%)**	**Peak Temperature**	**Experimental Resolution (Ratio of AHE active sites vs available sites)**	**AHE?**
BE3323	$PdD_{1.0}$	1204 °C	2.9E-8	No
BE3861	$Pd_{75}Rh_{25}D_x$	1186 °C	9.0E-8	No
BE3801	$Pd_{75}Ni_{25}D_x$	901 °C	7.0E-8	No
BE3822	$Pd_{75}Ag_{25}D_x$	879 °C	6.2E-8	No
BE3829	$Pd_{75}Pt_{25}D_x$	1204 °C	4.7E-8	No
BE3845	$Pd_{92.5}B_{7.5}D_x$	945 °C	6.1E-8	No

BE3922	NiD_x	1086 °C	6.8E-8	No

Table 1 : Key TI12 experiments

Across our TI12 campaign, we repeated the above protocol and analysis with several materials, including many Pd alloys, to investigate the potential role of alternate atomic species. Table 1 shows this data, along with the experimental peak temperatures (determined based on the known melting temperatures: all samples are stimulated in excess of melting). In each case, we determine the experimental resolution in terms of how many AHE events would need to happen to be observable. **In the worst-case scenario, 1 in 100 million potential AHE sites would have to undergo AHE to be observable**. In other words, our TI12 campaign places a lower limit and suggests that *if* AHE were to be occurring, it is happening in less than 1 in 100 million potential cases.

To further support the accuracy of our TI12 apparatus and the above claim regarding the lack of AHE, we confirmed our resolution by using a known, thermally activated exothermic reaction (i.e., a non-nuclear means of generating "excess" heat). To confirm our resolution (i.e.., adiabatic assumption), and experimentally generate error bounds, we performed a TI12 experiment using a 50 / 50 at% mix of Pd and Al powder in place of PdD_x, where the creation of the intermetallic alloy is an exothermic reaction; this is akin to thermite without relying on oxygen transfer and occurs under high vacuum. This control experiment reacts the $Pd_{50}Al_{50}$ alloy to completion, with an expected exothermic reaction of 175 kJ/mol. Based on the known mass added, we anticipate 19.5 J of generated additional heat from the exothermic reaction. Indeed, we measure 21.9 J as "excess" heat in our experiment, or approximately 12% error between the measured and expected value.

Across all TI campaigns, we have rigorously tested nearly 12 orders of magnitude in pressure conditions, ranging from ultrahigh vacuum to 1 GPa. We've exceeded the melting temperature of PdD and PdH, directly measuring 100% loading for both isotopes. We have also expanded our search to other materials and alloys. We have done all of the above while maximizing our system resolution, requiring as little as 10^{-6} per-cent of the AHE sites to be active for us to unambiguously detect AHE, exceeding the resolution of the best available calorimeters available. This parameter space is highlighted below in Fig. 13, but concludes that, under these conditions, **we unfortunately have not seen any discernible evidence of AHE in our Thermal Ignition experiments**.

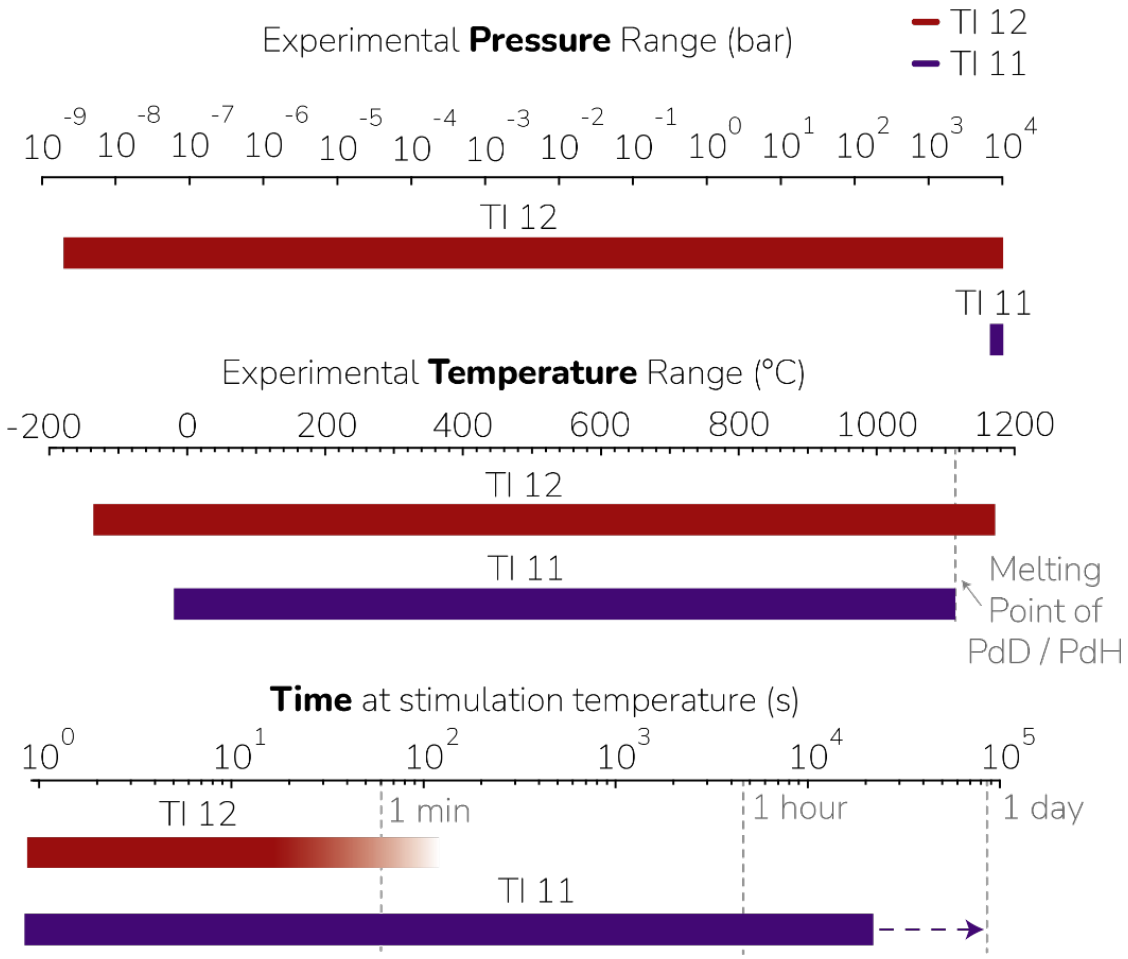

Figure 13: Parameter space explored across TI campaigns. Multiple orders of magnitudes on various experimental conditions were varied, in addition to the material list shown in the above table.